

Contribution of vector resonances to the $\bar{B}_d^0 \rightarrow \bar{K}^{*0} \mu^+ \mu^-$ decay

Alexander Yu. Korchin^{a,1,2}, Vladimir A. Kovalchuk^{b,1}

¹NSC ‘Kharkov Institute of Physics and Technology’, 61108 Kharkiv, Ukraine

²V.N. Karazin Kharkiv National University, 61022 Kharkiv, Ukraine

Received: date / Accepted: date

Abstract The fully differential angular distribution for the rare flavor-changing neutral current decay $\bar{B}_d^0 \rightarrow \bar{K}^{*0} (\rightarrow K^- \pi^+) \mu^+ \mu^-$ is studied. The emphasis is placed on accurate treatment of the contribution from the processes $\bar{B}_d^0 \rightarrow \bar{K}^{*0} (\rightarrow K^- \pi^+) V$ with intermediate vector resonances $V = \rho(770), \omega(782), \phi(1020), J/\psi, \psi(2S), \dots$ decaying into the $\mu^+ \mu^-$ pair. The dilepton invariant-mass dependence of the branching ratio, longitudinal polarization fraction f_L of the \bar{K}^{*0} meson, and forward-backward asymmetry A_{FB} is calculated and compared with data from Belle, CDF and LHCb. It is shown that inclusion of the resonance contribution may considerably modify the branching ratio, calculated in the SM without resonances, even in the invariant-mass region far from the so-called charmonia cuts applied in the experimental analyses. This conclusion crucially depends on values of the unknown phases of the $B^0 \rightarrow K^{*0} J/\psi$ and $B^0 \rightarrow K^{*0} \psi(2S)$ decay amplitudes with zero helicity.

PACS 13.20.He; · 13.25.Hw; · 12.40.Vv

1 Introduction

The investigation of the rare decay

$$\bar{B}_d^0 \rightarrow \bar{K}^{*0} (\rightarrow K^- \pi^+) \mu^+ \mu^-$$

induced by the flavor-changing neutral current (FCNC) transition $b \rightarrow s \mu^+ \mu^-$ is an important test of the standard model (SM) and its extensions (see [1] for a review). The phenomenology of this decay mode has been discussed by many authors, e.g. see Refs. [2–27].

^ae-mail: korchin@kipt.kharkov.ua

^be-mail: koval@kipt.kharkov.ua

This decay takes place in a very wide region of dimuon invariant mass squared, $q^2 = (q_+ + q_-)^2$, namely $4m_\mu^2 \leq q^2 \leq q_{\max}^2 = (m_B - m_{K^*})^2$. The light vector resonances $\rho(770), \omega(782), \phi(1020)$ (and their radial excitations) and the $c\bar{c}$ resonances $J/\psi, \psi(2S)$ (and higher states) are also located in this region. Thus at $q^2 \approx m_V^2$ the decay $\bar{B}_d^0 \rightarrow \bar{K}^{*0} \mu^+ \mu^-$ can go through the hadronic weak decay $\bar{B}_d^0 \rightarrow \bar{K}^{*0} V$, followed by the dimuonic annihilation of vector meson V . All resonances with $m_V < m_B - m_{K^*}$ make a contribution to this mechanism. Therefore both the nonresonant and resonant parts can contribute to the total amplitude of the decay $\bar{B}_d^0 \rightarrow \bar{K}^{*0} \mu^+ \mu^-$.

Main attention in literature has been paid to description of the nonresonant amplitude of the decay $\bar{B}_d^0 \rightarrow \bar{K}^{*0} \mu^+ \mu^-$ in the region $1 \text{ GeV}^2 \leq q^2 \leq 6 \text{ GeV}^2$. In this region, using the QCD factorization (QCdf) [28, 29], one can perform a systematical calculation of non-factorizable corrections to “naive factorization approximation” (NFA) and spectator effects [30, 31]. At larger dimuon masses, at about $q^2 > 14 \text{ GeV}^2$, the QCdf and the light-cone sum rules (LCSR) methods are not applicable. For the estimation of non-factorizable corrections, an operator product expansion in powers of $1/\sqrt{q^2}$ can be used [32, 33]. In the region $10 \text{ GeV}^2 \lesssim q^2 \lesssim 13 \text{ GeV}^2$ the non-factorizable effects due to soft-gluon emission have been included in [34].

Often the resonant contribution to amplitudes of rare decays of B -meson is modeled in terms of the Breit-Wigner functions for the resonances [35–39]. In these references the resonance corrections are added to the perturbative loops of charm quarks. Note an original approach of Ref. [40] for the inclusive $B \rightarrow X_s \ell^+ \ell^-$ process, in which dispersion relation exploiting experimentally measured cross section $\sigma(e^+e^- \rightarrow \text{hadrons})$

has been applied to account for the resonance terms (see also [41]).

These approaches more often apply to the inclusive decays $B \rightarrow X_s \ell^+ \ell^-$ and use information on the $B \rightarrow X_s J/\psi$ and $B \rightarrow X_s \psi(2S)$ branching ratios for description of the resonant contribution. Sometimes, such approaches are extended to the exclusive decays $B \rightarrow K(K^*) \ell^+ \ell^-$ [4, 38, 39], in which the branching ratios for exclusive decays $B \rightarrow K(K^*) J/\psi$ and $B \rightarrow K(K^*) \psi(2S)$ are used. In these studies, carried out in framework of the NFA, additional factors k_V are introduced into the resonant terms to adjust the branching ratios for the decays, for instance,

$$\begin{aligned} BR(B \rightarrow K^* V \rightarrow K^* \ell^+ \ell^-) \\ = BR(B \rightarrow K^* V) BR(V \rightarrow \ell^+ \ell^-), \end{aligned}$$

where the right-hand side is taken from experiment.

Recall that, in general, the process $B \rightarrow K^* V$ is characterized not only by the branching ratio. The decay of a B_d^0 meson into a pair of vector mesons, $B_d^0 \rightarrow K^{*0} V$, is described by three complex amplitudes [42]. In the transverse basis [43, 44], these decay amplitudes correspond to linearly polarized states of vector mesons, which are polarized either longitudinally (0) or transversely to the direction of their motion, being polarized in parallel (\parallel) or perpendicular (\perp) to each another. Overall, six real parameters describe three complex amplitudes A_0^V , A_{\parallel}^V , and A_{\perp}^V . They could be chosen to be, for example, the branching ratio, $|A_0^V|^2$, $|A_{\parallel}^V|^2$, $\arg(A_{\parallel}^V/A_0^V)$, $\arg(A_{\perp}^V/A_0^V)$ and one overall phase $\arg(A_0^V)$. The phase convention is arbitrary for an isolated decay $B_d^0 \rightarrow K^{*0} V$. Sometimes, this phase is chosen zero, $\arg(A_0^V) = 0$. However, for certain B decays, this phase can produce meaningful and observable effects, such as for $B \rightarrow V K_J^*$ with $J = 0, 1, 2, \dots$

For example, in the decay $B_d^0 \rightarrow K^{*0} \phi$, the phase of the amplitude A_0^{ϕ} has been measured with respect to the phase of the amplitude A_{00}^{ϕ} of the decay $B_d^0 \rightarrow K_0^{*0}(1430) \phi$ and is equal to $\arg(A_{00}^{\phi}/A_0^{\phi}) = 2.82 \pm 0.15 \pm 0.09$ [45, 46]. For the other vector resonances V , the corresponding relative phase has not been measured so far.

At present in decay modes to the light resonances, $B_d^0 \rightarrow K^{*0} \rho(770)$ and $B_d^0 \rightarrow K^{*0} \omega(782)$, only the branching ratio and longitudinal polarization fraction of the K^* meson are measured, while the decays to radial excitations, $\omega(1420)$, $\rho(1450)$, $\omega(1650)$, $\rho(1700)$, \dots , have not been observed. At the same time, all amplitudes of the decay $B_d^0 \rightarrow K^{*0} \phi(1020)$ are known from experiment, while there is no information on B decays to radial excitations of $\phi(1020)$. For the $B_d^0 \rightarrow K^{*0} J/\psi$ and $B_d^0 \rightarrow K^{*0} \psi(2S)$ decays, the full angular analysis has been performed. As for the decays to the

higher states, $\psi(3770)$, $\psi(4040)$, $\psi(4160)$, $\psi(4415)$, the experimental information is absent.

In the present paper for description of resonant contribution to the four-body decay $\bar{B}_d^0 \rightarrow K^- \pi^+ \mu^+ \mu^-$ the available information on the helicity amplitudes for $B \rightarrow K^* V$ is used. The fully differential angular distribution over the three angles and dimuon invariant mass is analyzed in the whole region $4m_{\mu}^2 \leq q^2 \leq (m_B - m_{K^*})^2$. The amplitude of this decay consists of the nonresonant amplitude in the SM model and the resonant amplitude. For the first amplitude we use the NFA, in which hadronic matrix elements are parameterized in terms of form factors [47], and the Wilson coefficients are taken in the next-to-next-to-leading order (NNLO) approximation.

The resonant amplitude is expressed in terms of the invariant amplitudes $S_{1,2,3}^V$ for the decays $B_d^0 \rightarrow K^{*0} V$. The information on the latter is taken from experiment if available, or from theoretical estimations. As mentioned above, the phase $\delta_0^V \equiv \arg(A_0^V)$ for an isolated decay $B_d^0 \rightarrow K^{*0} V$ is arbitrary. This phase may produce observable effects in the decay $\bar{B}_d^0 \rightarrow \bar{K}^{*0} \mu^+ \mu^-$ via the interference with the nonresonant amplitude. We investigate influence of the phases δ_0^V for each resonance V on the differential branching ratio, longitudinal polarization fraction f_L of K^* and forward-backward asymmetry A_{FB} .

We also study two aspects of the resonant amplitude. The first one is related to the fact that the vector mesons are off their mass shells, therefore an off-mass-shell extension of the on-mass-shell $B_d^0 \rightarrow K^{*0} V$ amplitudes is proposed. The second one is the choice of the vector-meson-dominance (VMD) model which describes the transition vertex $V \gamma$. We use two versions of the VMD model (called further VMD1 and VMD2) which result in rather different $V \gamma$ vertices. In particular, in the VMD2 model, the $V \gamma$ vertex is suppressed compared to the VMD1 vertex in the region $q^2 \ll m_V^2$.

Results of the present calculations are compared with the recent data from Belle, CDF and LHCb experiments. Usually in these experiments the $c\bar{c}$ resonance contributions are removed by putting cuts on the invariant dimuon mass near the resonance mass $q^2 = m_V^2$. This assumption is used in the analyses of all ongoing and planned experiments.

The paper is organized as follows. In Section 2.1 the fully differential angular distribution is discussed. Nonresonant and resonant amplitudes in the transverse basis are specified in Section 2.2. Results for the dependence of observables on the invariant mass squared are presented in Section 3. Conclusions are drawn in Section 4. In Appendix A calculation of the $B^0 \rightarrow K^{*0} V$

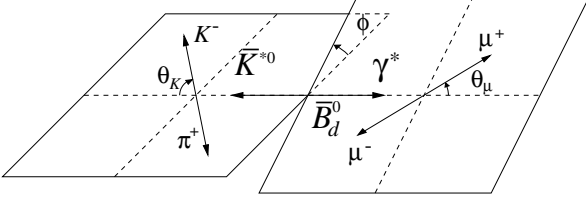


Fig. 1 Definition of helicity angles θ_μ , θ_K , and ϕ , for the decay $\bar{B}_d^0 \rightarrow \bar{K}^{*0} \mu^+ \mu^-$.

amplitudes for the off-mass-shell vector meson V is described.

2 Angular distributions and amplitudes for the $\bar{B}_d^0 \rightarrow \bar{K}^{*0} \mu^+ \mu^-$ decay

2.1 Differential decay rate

The decay $\bar{B}_d^0 \rightarrow \bar{K}^{*0} \mu^+ \mu^-$, with $\bar{K}^{*0} \rightarrow K^- \pi^+$ on the mass shell¹, is completely described by four independent kinematic variables: the dimuon invariant mass squared, q^2 , and the three angles θ_μ , θ_K , ϕ . In the helicity frame (Fig. 1), the angle θ_μ (θ_K) is defined as the angle between the directions of motion of μ^+ (K^-) in the γ^* (\bar{K}^{*0}) rest frame and the γ^* (\bar{K}^{*0}) in the \bar{B}_d^0 rest frame. The azimuthal angle ϕ is defined as the angle between the decay planes of $\gamma^* \rightarrow \mu^+ \mu^-$ and $\bar{K}^{*0} \rightarrow K^- \pi^+$ in the \bar{B}_d^0 rest frame. The differential decay rate in these coordinates is given by

$$\frac{d^4 \Gamma}{dq^2 d \cos \theta_\mu d \cos \theta_K d \phi} = \beta_\mu m_B N^2 \hat{q}^2 \sqrt{\hat{\lambda}} \frac{9}{64 \pi} \sum_{k=1}^{11} a_k(q^2) g_k(\theta_\mu, \theta_K, \phi), \quad (1)$$

where the angular terms g_k are defined as

$$\begin{aligned} g_1 &= 4 \sin^2 \theta_\mu \cos^2 \theta_K, g_2 = (1 + \cos^2 \theta_\mu) \sin^2 \theta_K, \\ g_3 &= \sin^2 \theta_\mu \cos 2\phi \sin^2 \theta_K, \\ g_4 &= -2 \sin^2 \theta_\mu \sin^2 \theta_K \sin 2\phi, \\ g_5 &= -\sqrt{2} \sin 2\theta_\mu \sin 2\theta_K \cos \phi, \\ g_6 &= -\sqrt{2} \sin 2\theta_\mu \sin 2\theta_K \sin \phi, g_7 = 4 \cos \theta_\mu \sin^2 \theta_K, \\ g_8 &= -2\sqrt{2} \sin \theta_\mu \sin 2\theta_K \cos \phi, \\ g_9 &= -2\sqrt{2} \sin \theta_\mu \sin 2\theta_K \sin \phi, \\ g_{10} &= 2 \cos^2 \theta_K, g_{11} = \sin^2 \theta_K, \end{aligned}$$

¹This means the narrow-width approximation for the \bar{K}^{*0} propagator: $(k^2 - m_{K^*}^2 + im_{K^*} \Gamma_{K^*})^{-1} \approx -i\pi \delta(k^2 - m_{K^*}^2)$.

and the amplitude terms a_k as

$$\begin{aligned} a_1 &= \beta_\mu^2 |A_0|^2, a_2 = \beta_\mu^2 (|A_{\parallel}|^2 + |A_{\perp}|^2), \\ a_3 &= \beta_\mu^2 (|A_{\perp}|^2 - |A_{\parallel}|^2), a_4 = \beta_\mu^2 \text{Im}(A_{\parallel} A_{\perp}^*), \\ a_5 &= \beta_\mu^2 \text{Re}(A_0 A_{\parallel}^*), a_6 = \beta_\mu^2 \text{Im}(A_0 A_{\perp}^*), \\ a_7 &= \beta_\mu \text{Re}(A_{\parallel L} A_{\perp L}^* - A_{\parallel R} A_{\perp R}^*), \\ a_8 &= \beta_\mu \text{Re}(A_{0L} A_{\perp L}^* - A_{0R} A_{\perp R}^*), \\ a_9 &= \beta_\mu \text{Im}(A_{0L} A_{\parallel L}^* - A_{0R} A_{\parallel R}^*), \\ a_{10} &= (1 - \beta_\mu^2) (|A_{0L} + A_{0R}|^2 + |A_t|^2), \\ a_{11} &= (1 - \beta_\mu^2) (|A_{\parallel L} + A_{\parallel R}|^2 + |A_{\perp L} + A_{\perp R}|^2), \end{aligned}$$

where $\beta_\mu \equiv \sqrt{1 - 4m_\mu^2/q^2}$, m_μ is the mass of the muon, m_B is the mass of the B_d^0 meson, $\hat{q}^2 \equiv q^2/m_B^2$, and

$$A_i A_j^* \equiv A_{iL}(q^2) A_{jL}^*(q^2) + A_{iR}(q^2) A_{jR}^*(q^2).$$

Here $i, j = (0, \parallel, \perp)$, the a_k dependent on products of the six transversity amplitudes $A_{0L(R)}$, $A_{\parallel L(R)}$ and $A_{\perp L(R)}$, where L and R refer to the chirality of the leptonic current, as well as the seventh transversity amplitude A_t . The latter amplitude is related to the time-like component of the virtual gauge boson, which does not contribute to the decay rate in the case of massless leptons and can be neglected if the lepton mass is small in comparison to the invariant-mass of the leptonic pair. Further, $\hat{\lambda} \equiv \lambda(1, \hat{q}^2, \hat{m}_{K^*}^2) = (1 - \hat{q}^2)^2 - 2(1 + \hat{q}^2) \hat{m}_{K^*}^2 + \hat{m}_{K^*}^4$, $\hat{m}_{K^*} \equiv m_{K^*}/m_B$, where m_{K^*} is the mass of the K^{*0} meson, and

$$N = |V_{tb} V_{ts}^*| \frac{G_F m_B^2 \alpha_{\text{em}}}{32 \pi^2 \sqrt{3} \pi}.$$

Here, V_{ij} are the Cabibbo-Kobayashi-Maskawa (CKM) matrix elements [48, 49], G_F is the Fermi coupling constant, α_{em} is the electromagnetic fine-structure constant.

The longitudinal, parallel, and perpendicular partial widths are given, respectively, by

$$\frac{d\Gamma_L}{dq^2} = m_B N^2 \beta_\mu \hat{q}^2 \sqrt{\hat{\lambda}} \left(\beta_\mu^2 |A_0|^2 + \frac{3m_\mu^2}{q^2} (|A_t|^2 + |A_{0L} + A_{0R}|^2) \right). \quad (2)$$

$$\frac{d\Gamma_{\parallel}}{dq^2} = m_B N^2 \beta_\mu \hat{q}^2 \sqrt{\hat{\lambda}} \left(\beta_\mu^2 |A_{\parallel}|^2 + \frac{3m_\mu^2}{q^2} |A_{\parallel L} + A_{\parallel R}|^2 \right). \quad (3)$$

$$\frac{d\Gamma_{\perp}}{dq^2} = m_B N^2 \beta_\mu \hat{q}^2 \sqrt{\hat{\lambda}} \left(\beta_\mu^2 |A_{\perp}|^2 + \frac{3m_\mu^2}{q^2} |A_{\perp L} + A_{\perp R}|^2 \right). \quad (4)$$

The familiar muon-pair invariant-mass spectrum for $\bar{B}_d^0 \rightarrow \bar{K}^{*0} \mu^+ \mu^-$ decay can be recovered after integration over all angles as

$$\frac{d\Gamma}{d\hat{q}^2} = \frac{d\Gamma_L}{d\hat{q}^2} + \frac{d\Gamma_{\parallel}}{d\hat{q}^2} + \frac{d\Gamma_{\perp}}{d\hat{q}^2}. \quad (5)$$

The fraction of K^* meson polarization is $[i = (L, \parallel, \perp)]$

$$f_i(q^2) = \frac{d\Gamma_i}{d\hat{q}^2} / \frac{d\Gamma}{d\hat{q}^2}.$$

Integrating Eq. (1) over the variables $\cos \theta_{\mu}$ and ϕ , we obtain

$$\begin{aligned} \frac{d^2 \Gamma}{d\hat{q}^2 d \cos \theta_K} &= \frac{d\Gamma}{d\hat{q}^2} \left(\frac{3}{2} f_L \cos^2 \theta_K \right. \\ &\quad \left. + \frac{3}{4} (1 - f_L) (1 - \cos^2 \theta_K) \right). \end{aligned} \quad (6)$$

Integration of Eq. (1) over $\cos \theta_K$ and ϕ yields

$$\begin{aligned} \frac{d^2 \Gamma}{d\hat{q}^2 d \cos \theta_{\mu}} &= m_B N^2 \beta_{\mu} \hat{q}^2 \sqrt{\lambda} \frac{3}{8} \left(2 \beta_{\mu}^2 |A_0|^2 \sin^2 \theta_{\mu} \right. \\ &\quad \left. + \beta_{\mu}^2 (|A_{\parallel}|^2 + |A_{\perp}|^2) (1 + \cos^2 \theta_{\mu}) + \frac{4m_{\mu}^2}{q^2} (|A_t|^2 \right. \\ &\quad \left. + |A_{0L} + A_{0R}|^2 + |A_{\parallel L} + A_{\parallel R}|^2 \right. \\ &\quad \left. + |A_{\perp L} + A_{\perp R}|^2) \right) + \frac{dA_{\text{FB}}^{(\mu)}}{d\hat{q}^2} \cos \theta_{\mu}, \end{aligned} \quad (7)$$

where $dA_{\text{FB}}^{(\mu)}/d\hat{q}^2$ is the muon forward-backward asymmetry,

$$\begin{aligned} \frac{dA_{\text{FB}}^{(\mu)}}{d\hat{q}^2} &\equiv \int_{-1}^1 \text{sgn}(\cos \theta_{\mu}) \frac{d^2 \Gamma}{d\hat{q}^2 d \cos \theta_{\mu}} d \cos \theta_{\mu} \\ &= m_B N^2 \beta_{\mu}^2 \hat{q}^2 \sqrt{\lambda} \frac{3}{2} \text{Re} (A_{\parallel L} A_{\perp L}^* - A_{\parallel R} A_{\perp R}^*), \end{aligned} \quad (8)$$

and the normalized forward-backward asymmetry $d\bar{A}_{\text{FB}}^{(\mu)}/d\hat{q}^2$ is given as

$$\frac{d\bar{A}_{\text{FB}}^{(\mu)}}{d\hat{q}^2} \equiv \frac{dA_{\text{FB}}^{(\mu)}}{d\hat{q}^2} / \frac{d\Gamma}{d\hat{q}^2}. \quad (9)$$

Finally, the one-dimensional angular distribution in the angle ϕ between the lepton and meson planes takes the form

$$\begin{aligned} \frac{d^2 \Gamma}{d\hat{q}^2 d\phi} &= \frac{1}{2\pi} \frac{d\Gamma}{d\hat{q}^2} \left(1 + \frac{1}{2} (1 - f_L) A_{\text{T}}^{(2)} \cos 2\phi \right. \\ &\quad \left. - A_{\text{Im}} \sin 2\phi \right), \end{aligned} \quad (10)$$

$$A_{\text{T}}^{(2)} \equiv \left(\frac{d\tilde{\Gamma}_{\perp}}{d\hat{q}^2} - \frac{d\tilde{\Gamma}_{\parallel}}{d\hat{q}^2} \right) / \left(\frac{d\tilde{\Gamma}_{\perp}}{d\hat{q}^2} + \frac{d\tilde{\Gamma}_{\parallel}}{d\hat{q}^2} \right), \quad (11)$$

$$\frac{d\tilde{\Gamma}_{\perp(\parallel)}}{d\hat{q}^2} = m_B N^2 \beta_{\mu}^3 \hat{q}^2 \sqrt{\lambda} |A_{\perp(\parallel)}|^2, \quad (12)$$

$$A_{\text{Im}} \equiv m_B N^2 \beta_{\mu}^3 \hat{q}^2 \sqrt{\lambda} \text{Im}(A_{\parallel} A_{\perp}^*), \quad (13)$$

where the asymmetry $A_{\text{T}}^{(2)}(q^2)$ is sensitive to new physics from right-handed currents beyond the standard model, and the amplitude $A_{\text{Im}}(q^2)$ is sensitive to complex phases in the hadronic matrix elements. Sometimes $A_{\text{T}}^{(2)}(q^2)$ is called transverse asymmetry [7].

2.2 Resonant and nonresonant transverse amplitudes

The effects of the long-distance contribution from the decays $\bar{B}_d^0 \rightarrow \bar{K}^{*0} V$, where $V = \rho^0, \omega, \phi, J/\psi(1S), \psi(2S), \dots$ mesons, followed by $V \rightarrow \mu^+ \mu^-$ in the decay $\bar{B}_d^0 \rightarrow \bar{K}^{*0} \mu^+ \mu^-$ are included through the VMD approach, as shown in Fig. 2. There is no unique way



Fig. 2 Nonresonant and resonant contributions to the decay amplitude.

of introducing the $V \gamma$ transition, and one can use various versions of VMD models which yield different $V \gamma$ transition vertices. In one of VMD models (see [50], chapter 6)

$$\langle \gamma(q); \mu | V(q); \nu \rangle = -e f_V Q_V m_V g^{\mu\nu}, \quad (14)$$

where $g^{\mu\nu}$ is the metric tensor, q is the photon (meson) four-momentum and Q_V is the effective electric charge of the quarks in the meson V :

$$\begin{aligned} Q_{\rho} &= \frac{1}{\sqrt{2}}, & Q_{\omega} &= \frac{1}{3\sqrt{2}}, & Q_{\phi} &= -\frac{1}{3}, \\ Q_{J/\psi} &= Q_{\psi(2S)} = \dots = \frac{2}{3}. \end{aligned} \quad (15)$$

The decay constant of the neutral vector meson f_V can be extracted from electromagnetic decay width, using

$$\Gamma_{V \rightarrow e^+ e^-} = \frac{4\pi \alpha_{em}^2}{3 m_V} f_V^2 Q_V^2. \quad (16)$$

We will call this version VMD1. The vertex in Eq. (14) follows from the transition Lagrangian

$$\mathcal{L}_{\gamma V} = -e f_V Q_V m_V A^{\mu} V_{\mu}. \quad (17)$$

Another model (called hereafter VMD2) originates from

$$\mathcal{L}_{\gamma V} = -\frac{e f_V Q_V}{2m_V} F^{\mu\nu} V_{\mu\nu}, \quad (18)$$

where $V_{\mu\nu} \equiv \partial_\mu V_\nu - \partial_\nu V_\mu$ and $F^{\mu\nu} \equiv \partial^\mu A^\nu - \partial^\nu A^\mu$. An advantage of the Lagrangian (18) is its explicit gauge-invariant form. Eq. (18) gives rise to the $V\gamma$ transition vertex

$$\langle \gamma(q); \mu | V(q); \nu \rangle = -\frac{ef_V Q_V}{m_V} (q^2 g^{\mu\nu} - q^\mu q^\nu), \quad (19)$$

The term $\propto q^\mu q^\nu$ does not contribute being contracted with the leptonic current $e\bar{u}(q_-)\gamma_\mu v(q_+)$, and vertex (19) is suppressed compared to (14) at small $q^2 \ll m_V^2$, i.e. in the region far from the vector-meson mass shell. Of course on the mass shell, $q^2 = m_V^2$, the VMD2 and VMD1 are equivalent.

These two versions of VMD model have been discussed earlier in Refs. [51, 52]. Note also that VMD2 vertex follows from the Resonance Chiral Theory [53] and has been applied [54] when studying the reaction $e^+e^- \rightarrow \pi^0\pi^0(\eta)\gamma$.

Parameters of vector resonances are collected in Table 1.

The nonresonant amplitudes are calculated in the NFA, with the short-distance NNLO Wilson coefficients, and nonperturbative $B \rightarrow K^*$ transition form factors.

Then the total amplitudes including nonresonant and resonant parts take the form

$$\begin{aligned} A_{0L,R} = & \frac{1}{2\hat{m}_{K^*}\sqrt{\hat{q}^2}} \left(C_0(q^2) (C_{9V}^{\text{eff}} \mp C_{10A}) \right. \\ & + 2\hat{m}_b (C_{7\gamma}^{\text{eff}} - C_{7\gamma}'^{\text{eff}}) \kappa_0(q^2) \\ & + 8\pi^2 \sum_V C_V D_V^{-1}(\hat{q}^2) \left((1 - \hat{q}^2 - \hat{m}_{K^*}^2) S_1^V \right. \\ & \left. \left. + \hat{\lambda} \frac{S_2^V}{2} \right) \right), \quad (20) \end{aligned}$$

$$\begin{aligned} A_{\parallel L,R} = & -\sqrt{2} \left(C_{\parallel}(q^2) (C_{9V}^{\text{eff}} \mp C_{10A}) \right. \\ & + 2\frac{\hat{m}_b}{\hat{q}^2} (C_{7\gamma}^{\text{eff}} - C_{7\gamma}'^{\text{eff}}) \kappa_{\parallel}(q^2) \\ & \left. + 8\pi^2 \sum_V C_V D_V^{-1}(\hat{q}^2) S_1^V \right), \quad (21) \end{aligned}$$

$$\begin{aligned} A_{\perp L,R} = & \sqrt{2}\hat{\lambda} \left(C_{\perp}(q^2) (C_{9V}^{\text{eff}} \mp C_{10A}) \right. \\ & + 2\frac{\hat{m}_b}{\hat{q}^2} (C_{7\gamma}^{\text{eff}} + C_{7\gamma}'^{\text{eff}}) \kappa_{\perp}(q^2) \\ & \left. + 4\pi^2 \sum_V C_V D_V^{-1}(\hat{q}^2) S_3^V \right), \quad (22) \end{aligned}$$

$$A_t = -2\sqrt{\frac{\hat{\lambda}}{\hat{q}^2}} C_{10A} A_0(q^2), \quad (23)$$

where

$$D_V(\hat{q}^2) = \hat{q}^2 - \hat{m}_V^2 + i\hat{m}_V \hat{\Gamma}_V(\hat{q}^2)$$

is the usual Breit-Wigner function for the V meson resonance shape with the energy-dependent width $\Gamma_V(q^2)$ [$\hat{\Gamma}_V(\hat{q}^2) = \Gamma_V(q^2)/m_B$], $\hat{m}_V \equiv m_V/m_B$, $\hat{\Gamma}_V \equiv \Gamma_V/m_B$, $m_V(\Gamma_V)$ is the mass (width) of a V meson and the form factors enter as

$$\begin{aligned} C_0(q^2) = & (1 - \hat{q}^2 - \hat{m}_{K^*}^2)(1 + \hat{m}_{K^*})A_1(q^2) \\ & - \hat{\lambda} \frac{A_2(q^2)}{1 + \hat{m}_{K^*}}, \quad (24) \end{aligned}$$

$$C_{\parallel}(q^2) = (1 + \hat{m}_{K^*})A_1(q^2), \quad (25)$$

$$C_{\perp}(q^2) = \frac{V(q^2)}{1 + \hat{m}_{K^*}}, \quad (26)$$

$$\begin{aligned} \kappa_0(q^2) \equiv & \left((1 - \hat{q}^2 + 3\hat{m}_{K^*}^2)(1 + \hat{m}_{K^*})T_2(q^2) \right. \\ & \left. - \frac{\hat{\lambda}}{1 - \hat{m}_{K^*}} T_3(q^2) \right) \left((1 - \hat{q}^2 - \hat{m}_{K^*}^2) \right. \\ & \left. \times (1 + \hat{m}_{K^*})^2 A_1(q^2) - \hat{\lambda} A_2(q^2) \right)^{-1}, \quad (27) \end{aligned}$$

$$\kappa_{\parallel}(q^2) \equiv \frac{T_2(q^2)}{A_1(q^2)} (1 - \hat{m}_{K^*}), \quad (28)$$

$$\kappa_{\perp}(q^2) \equiv \frac{T_1(q^2)}{V(q^2)} (1 + \hat{m}_{K^*}). \quad (29)$$

In the above formulas the definition $\hat{m}_b \equiv \overline{m}_b(\mu)/m_B$, $\hat{m}_s \equiv \overline{m}_s(\mu)/m_B$ are used, and $\overline{m}_b(\mu)$ [$\overline{m}_s(\mu)$] is the running bottom (strange) quark mass in the $\overline{\text{MS}}$ scheme at the scale μ .

The SM Wilson coefficients have been obtained in [13] at the scale $\mu = 4.8$ GeV to NNLO accuracy and equal

$$C_{7\gamma}^{\text{eff}}(\mu) = -0.304, \quad C_{9V}(\mu) = 4.211, \quad C_{10A}(\mu) = -4.103,$$

$C_{9V}^{\text{eff}} = C_{9V} + Y(q^2)$, where $Y(q^2)$ is quark-loop function given in Ref. [30]. Note that in the framework of the SM $\overline{m}_b(\mu) C_{7\gamma}^{\text{eff}} = \overline{m}_s(\mu) C_{7\gamma}'^{\text{eff}}$.

Further, $A_0(q^2)$, $A_1(q^2)$, $A_2(q^2)$, $V(q^2)$, $T_1(q^2)$, $T_2(q^2)$, $T_3(q^2)$ are the $B \rightarrow K^*$ transition form factors. In the numerical estimations, we use the form factors from the LCSR calculation [47].

In Eqs. (20)-(22), S_i^V ($i = 1, 2, 3$) are the invariant amplitudes of the decay $B_d^0 \rightarrow K^{*0} V$. These amplitudes are calculated in Appendix A. The coefficients C_V in the resonant contribution are

$$C_V = \frac{Q_V m_V f_V}{q^2} \text{ (VMD1)}, \quad C_V = \frac{Q_V f_V}{m_V} \text{ (VMD2)}.$$

Table 1 Mass, total width, leptonic decay width and coupling f_V of vector mesons [55] (experimental uncertainties are not shown).

V	$m_V(\text{MeV})$	$\Gamma_V(\text{MeV})$	$\Gamma_{V \rightarrow e^+ e^-}(\text{keV})$	$f_V(\text{MeV})$
ρ^0	775.49	149.1	7.04	221.2
ω	782.65	8.49	0.60	194.7
ϕ	1019.455	4.26	1.27	228.6
J/ψ	3096.916	0.0929	5.55	416.4
$\psi(2S)$	3686.09	0.304	2.35	295.6
$\psi(3770)$	3772.92	27.3	0.265	100.4
$\psi(4040)$	4039	80	0.86	187.2
$\psi(4160)$	4153	103	0.83	186.5
$\psi(4415)$	4421	62	0.58	160.8

Table 2 The numerical input used in our analysis.

$ V_{tb}V_{ts}^* = 0.04026$	$G_F = 1.16637 \times 10^{-5} \text{ GeV}^{-2}$
$\mu = m_b = 4.8 \text{ GeV}$	$\alpha_{\text{em}} = 1/137.036$
$m_c = 1.4 \text{ GeV}$	$m_B = 5.27950 \text{ GeV}$
$\bar{m}_b(\mu) = 4.14 \text{ GeV}$	$\tau_B = 1.525 \text{ ps}$
$\bar{m}_s(\mu) = 0.079 \text{ GeV}$	$m_{K^*} = 0.89594 \text{ GeV}$

The energy-dependent widths of light vector resonances ρ , ω and ϕ are chosen as in Ref. [14]. The updated branching ratios for resonances decays to different channels are taken from [55]. For the $c\bar{c}$ resonances J/ψ , $\psi(2S)$, ... we take the constant widths.

In order to calculate the resonant contribution to the amplitude of the $\bar{B}_d^0 \rightarrow \bar{K}^{*0} \mu^+ \mu^-$ decay, one has to know the amplitudes of the decays $\bar{B}_d^0 \rightarrow \bar{K}^{*0} \rho$, $\bar{B}_d^0 \rightarrow \bar{K}^{*0} \omega$, $\bar{B}_d^0 \rightarrow \bar{K}^{*0} \phi$, $\bar{B}_d^0 \rightarrow \bar{K}^{*0} J/\psi$, $\bar{B}_d^0 \rightarrow \bar{K}^{*0} \psi(2S)$. The information on the $\bar{B}_d^0 \rightarrow \bar{K}^{*0} \phi$, $\bar{B}_d^0 \rightarrow \bar{K}^{*0} J/\psi$, $\bar{B}_d^0 \rightarrow \bar{K}^{*0} \psi(2S)$ decays can be taken from experiment [55]. For the light resonances ρ and ω we use the theoretical prediction [56] for the decay amplitudes. At the same time, we are not aware of a similar prediction for the higher $c\bar{c}$ resonances, such as $\psi(3770)$ and so on, and therefore do not include these resonances.

The parameters of the model are indicated in Table 2.

3 Results of the calculation for the $\bar{B}_d^0 \rightarrow \bar{K}^{*0} \mu^+ \mu^-$ decay

In Figs. 3 and 4 we present results for the dependence of several observables in the $\bar{B}_d^0 \rightarrow \bar{K}^{*0} \mu^+ \mu^-$ decay on the dimuon invariant mass squared. The interval of q^2 is taken from $4m_\mu^2$ to $q_{\text{max}}^2 = (m_B - m_{K^*})^2 \approx 19.22 \text{ GeV}^2$.

In order to adequately compare results of calculations with experiments from Belle (KEKB) [57], CDF (Tevatron) [58, 59] and LHCb [60] we show the binned

Table 3 Experimental bins in q^2 used in the data analyses [60] (the first column), [57–59] (the second column) and in our calculation.

$q^2 \text{ (GeV}^2\text{)}$	$q^2 \text{ (GeV}^2\text{)}$
0.10 - 2.00	0.00 - 2.00
2.00 - 4.30	2.00 - 4.30
4.30 - 8.68	4.30 - 8.68
10.09 - 12.86	10.09 - 12.86
14.18 - 16.00	14.18 - 16.00
16.00 - 19.00	16.00 - q_{max}^2

predictions, i.e. the calculated values averaged over the experimental bins. These bins are indicated in Table 3.

The solid line demonstrate the prediction of the SM without resonances for the q^2 -dependence of all observables; the horizontal bars are the corresponding binned results.

The dashed rectangles in Figs. 3 and 4 show possible contributions of the intermediate vector resonances in each q^2 -bin. To obtain these rectangles the phases $\delta_0^V = \arg(A_0^V)$ of the $B \rightarrow K^*V$ decay amplitudes with the zero helicity for $V = \rho, \omega, \phi, J/\psi, \psi(2S)$ have been varied from 0 to 2π . The upper (lower) side of the rectangles corresponds to the maximal (minimal) value of the branching ratio in each bin. The dominant dependence on the phase δ_0^V comes from the $c\bar{c}$ resonances J/ψ and $\psi(2S)$, while the phase dependence for the ρ, ω and ϕ is of minor importance. This is explained by the much bigger contribution of the $c\bar{c}$ resonances compared to the light ones.

Predictions of the VMD1 and VMD2 models (Section 2.2) differ at relatively small q^2 . This is due to the fact that at small q^2 the high-lying resonances J/ψ and $\psi(2S)$ are far off their mass shells and in these kinematical conditions the VMD1 and VMD2 models give different results. On the contrary, in the high q^2 region, close to the mass shells for the $c\bar{c}$ resonances, the results with VMD1 and VMD2 do not differ.

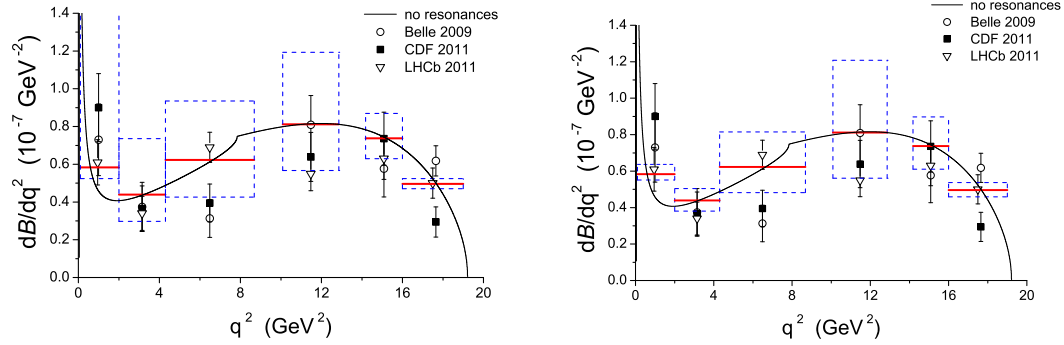


Fig. 3 Differential branching ratio as a function of q^2 . Solid lines correspond to calculation in the SM without resonances, and the horizontal bars (red online) are the corresponding binned (averaged over the experimental bins) results. In the first bin calculation is performed for $0.1 \text{ GeV}^2 < q^2 < 2.0 \text{ GeV}^2$. The dashed rectangles (blue online) show contribution of the intermediate resonances: left (right) panel - in the VMD1 (VMD2) model. The uncertainty of the resonance contribution is related to the unknown phase δ_0^V of the resonance amplitudes (see the text). The upper side of the resonance rectangle (left side) is located at 3.54 and is not shown. The form factors are taken from [47]. The data Belle (KEKB) [57], CDF (Tevatron) [58, 59] and LHCb [60] are shown by the circles, filled boxes and triangles respectively (the horizontal error bars are not shown - they are given in Table 3).

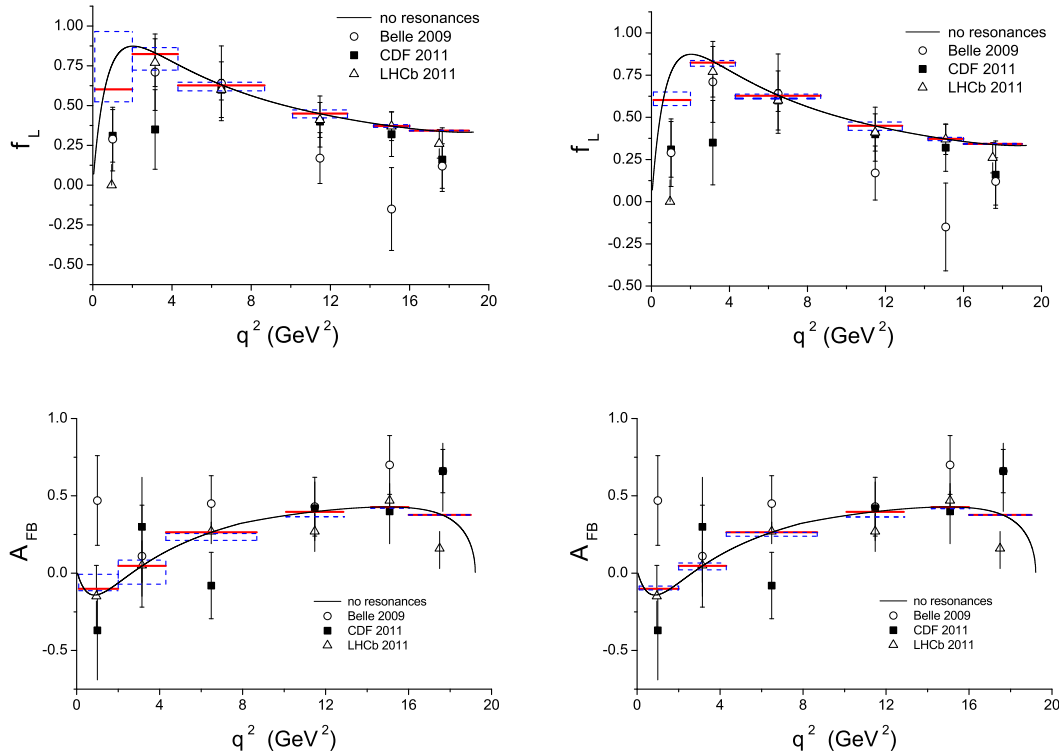


Fig. 4 Longitudinal polarization fraction of K^* meson (upper panel) and forward-backward asymmetry A_{FB} (lower panel) as functions of q^2 . Due to the choice of reference frame in Fig. 1, the forward-backward asymmetry A_{FB} in Refs. [57–60] is related to asymmetry in Eq. (9) via $A_{FB} = -d\bar{A}_{FB}^{(\mu)}/dq^2$. The other notation is the same as in Fig. 3.

In the experimental analyses certain cuts in q^2 are applied in order to suppress the charmonia contributions (the so-called charmonia veto). Correspondingly in Figs. 3 and 4 we also use these cuts. As it is seen from Fig. 3, the charmonia resonances may contribute to the differential branching far beyond their pole positions and beyond the charmonia veto, although their contribution crucially depends on the values of the zero-helicity phases $\delta_0^{J/\psi}$ and $\delta_0^{\psi(2S)}$. The observed in the VMD1 model sizable contribution of the $c\bar{c}$ -resonances at small values of q^2 occurs at certain values of these phases. Of course there exist values of $\delta_0^{J/\psi}$ and $\delta_0^{\psi(2S)}$ at which resonance contribution is small.

Comparing these results with results of Refs. [4, 38, 39] we note that in these papers the amplitudes of the decays $B \rightarrow K^* J/\psi$ and $B \rightarrow K^* \psi(2S)$ are calculated in framework of the NFA which implies zero phases. In contrast, our calculation is free from this limitation since the amplitudes are taken from experiment and thus the phases δ_0^V for all resonances V can be chosen arbitrary and independent.

Note that long-distance effects due to the nonfactorizable soft-gluon emission from the c -quarks have been included in Ref. [34]. Authors have shown that these effects lead to a modification, depending on the K^* polarization, of the Wilson coefficient $C_{9V}(\mu)$. The form factors and the Wilson coefficients in [34] are different from the corresponding quantities in our calculation. In framework of this approach we estimated the differential branching ratio in the region $1.0 \text{ GeV}^2 < q^2 < 9.0 \text{ GeV}^2$, using the Wilson coefficients and form factors of our work. Results of this calculation along with results of the present work are shown in Table 4.

Table 4 Differential branching ratio averaged over the two experimental bins. Results in our approach with resonances (VMD1 and VMD2) show variation of the branching ratio depending on the phases δ_0^V . Values in the last row are obtained following approach [34] for the central values of all parameters in Eq. (70) from [34] without taking into account uncertainties.

	dB/dq^2 (10^{-7} GeV^{-2})	
q^2 (GeV^2)	2.00 - 4.30	4.30 - 8.68
SM without resonances	0.44	0.63
VMD1	0.30 - 0.74	0.43 - 0.94
VMD2	0.38 - 0.50	0.48 - 0.82
Ref. [34]	0.44	0.60

As is seen, results of both approaches are comparable, at least in these intervals of q^2 and for a certain choice of phases δ_0^V . Besides, our calculation in the SM without resonances in framework of the NFA turns out

to be relatively close to the calculation following approach of Ref. [34].

As expected, the observables which are the ratios of the bilinear combinations of the amplitudes, such as f_L or A_{FB} , are less sensitive to the phases of the resonance contribution (see Fig. 4). Moreover, the latter is generally small independently of δ_0^V , apart from the region of relatively small $q^2 \lesssim 4 \text{ GeV}^2$.

It should be noted that for the inclusive decay $B \rightarrow X_s e^+ e^-$, in Ref. [61] soft-gluon emission from the charm loop has been considered and long-distance corrections of $\mathcal{O}(\Lambda_{QCD}^2/m_c^2)$ to the differential branching and forward-backward asymmetry are shown to be small in the region away from the $c\bar{c}$ resonances. Although this inclusive process is amenable to clean theoretical description for $1 \text{ GeV}^2 < q^2 < 6 \text{ GeV}^2$ and $q^2 > 14.4 \text{ GeV}^2$ [62], the experimental information on differential branching ratio is still rather limited [63, 64]. The situation is not likely to improve in the nearest future. At the same time for the exclusive decays $B \rightarrow K^*(\rightarrow K\pi) \ell^+ \ell^-$ a high statistics is expected at LHCb, and this will allow for measurement of various observables in these processes. Therefore the exclusive decays have quite a good potential for tests of the SM and search for effects beyond the SM.

4 Conclusions

The rare FCNC decay $\bar{B}_d^0 \rightarrow \bar{K}^{*0}(\rightarrow K^- \pi^+) \mu^+ \mu^-$ has been studied in the whole region of muon-antimuon invariant masses. We performed calculations of the differential branching ratio, polarization fraction f_L of the K^* meson and forward-backward asymmetry A_{FB} for the four-body decay $\bar{B}_d^0 \rightarrow K^- \pi^+ \mu^+ \mu^-$. Main emphasis in our study is placed on contribution of the intermediate vector resonances in the process $\bar{B}_d^0 \rightarrow \bar{K}^{*0}(\rightarrow K^- \pi^+) V$ with $V = \rho(770), \omega(782), \phi(1020), J/\psi, \psi(2S)$, decaying into the $\mu^+ \mu^-$ pair. Various aspects of theoretical treatment of this long-distance contribution have been investigated.

One aspect is the choice of VMD model describing the $V\gamma$ transition. We applied two different versions called VMD1 and VMD2. In particular, VMD2 model explicitly obeys gauge invariance and the corresponding $V\gamma$ vertex is suppressed compared to the $V\gamma$ vertex in the VMD1 model at small values of the photon invariant mass, far from the vector-meson mass shell. This turns out to be important when calculating the contribution of the high-lying J/ψ and $\psi(2S)$ resonances to the branching ratio at $q^2 \ll m_V^2$.

Another aspect is the structure of the vertex $\bar{B}_d^0 \rightarrow \bar{K}^{*0} V$ with the off-shell vector meson. We used an off-mass-shell extension of the helicity amplitudes which

describe production of the on-shell vector mesons V . For the latter amplitudes all the experimentally available information is used, and otherwise theoretical predictions.

The calculations are compared with recent data [57–60] for the q^2 -dependence of the differential branching ratio, longitudinal polarization fraction of the K^* meson and forward-backward asymmetry. In these analyses the cuts around the pole positions of the charmonia resonances are applied to suppress these contributions (charmonia veto). Our calculation shows that the intermediate resonances may considerably modify the branching ratio, calculated in the SM without resonances in framework of the NFA, even in the q^2 -region located far from these cuts. Main contribution comes from the $c\bar{c}$ resonances J/ψ and $\psi(2S)$. This conclusion, however, crucially depends on values of the unknown zero-helicity phases $\delta_0^{J/\psi}$ and $\delta_0^{\psi(2S)}$ for the decays $B^0 \rightarrow K^{*0} J/\psi$ and $B^0 \rightarrow K^{*0} \psi(2S)$ respectively. In view of these results one should keep in mind that the resonance contribution may imitate effects of new physics, the search for which is one of the goals of current and planned experiments on BaBar, CDF, Belle and LHCb.

As for the observables f_L and A_{FB} , these are less sensitive to the phases of the resonance contribution and moreover the latter is generally small independently of δ_0^V (apart from the region of relatively small $q^2 \lesssim 4$ GeV² in the VMD1 model). Apparently data for these observables are more appropriate for adequate comparison with the prediction of the SM without resonances.

Appendix A: Amplitudes of $B \rightarrow K^*V$ decays

An important ingredient of the resonant contribution is amplitude of the decay of B meson into two vector mesons, $B(p) \rightarrow V_1(q, \epsilon_1) + V_2(k, \epsilon_2)$, with on-mass-shell meson V_2 ($k^2 = m_2^2$) and off-mass-shell meson V_1 ($q^2 \neq m_1^2$). For the case of two on-mass-shell final mesons one can write the amplitude in the form [42]

$$\mathcal{M} = \frac{G_F m_B^3}{\sqrt{2}} |V_{CKM}| \left(S_1 g_{\mu\nu} + \frac{S_2}{m_B^2} p_\mu p_\nu - i \frac{S_3}{m_B^2} \varepsilon_{\mu\nu\alpha\beta} q^\alpha k^\beta \right) \epsilon_1^{\mu*} \epsilon_2^{\nu*} \quad (\text{A.1})$$

in terms of three invariant amplitudes S_1 , S_2 and S_3 , V_{CKM} is a CKM factor. The quantities S_1 , S_2 and S_3 may be complex and involve two types of phases, CP -conserving strong phases and CP -violating weak phases. In general, the invariant amplitudes are a sum of several interfering amplitudes, S_{1j} , S_{2j} and S_{3j} , respectively.

Then the phase structure of S_1 , S_2 and S_3 is:

$$S_k = \sum_j |S_{kj}| e^{i\varphi_{kj}} e^{i\delta_{kj}} \quad (k = 1, 2, 3), \quad (\text{A.2})$$

where φ_{1j} , φ_{2j} , and φ_{3j} are the CP -violating weak phases and δ_{1j} , δ_{2j} , and δ_{3j} are the CP -conserving strong phases.

Using CPT invariance, we can represent the matrix element for the charge-conjugate decay $\bar{B}(p) \rightarrow \bar{V}_1(q, \epsilon_1) \bar{V}_2(k, \epsilon_2)$ as

$$\overline{\mathcal{M}} = \frac{G_F m_B^3}{\sqrt{2}} |V_{CKM}^*| \left(\bar{S}_1 g_{\mu\nu} + \frac{\bar{S}_2}{m_B^2} p_\mu p_\nu + i \frac{\bar{S}_3}{m_B^2} \varepsilon_{\mu\nu\alpha\beta} q^\alpha k^\beta \right) \epsilon_1^{\mu*} \epsilon_2^{\nu*}, \quad (\text{A.3})$$

where \bar{S}_1 , \bar{S}_2 , and \bar{S}_3 can be derived from S_1 , S_2 , and S_3 by reversing the sign of the CP -violating phase. Note that if the $B \rightarrow V_1 V_2$ decay is invariant under the CP symmetry, then $\bar{S}_1 = S_1$, $\bar{S}_2 = S_2$, and $\bar{S}_3 = S_3$. On the other hand, if all CP -conserving phases of invariant amplitudes are equal to zero, then $\bar{S}_1 = S_1^*$, $\bar{S}_2 = S_2^*$, and $\bar{S}_3 = S_3^*$.

The helicity amplitudes in terms of three invariant amplitudes, S_1 , S_2 , and S_3 are:

$$H_\lambda \equiv \left(S_1 g_{\mu\nu} + \frac{S_2}{m_B^2} p_\mu p_\nu - i \frac{S_3}{m_B^2} \varepsilon_{\mu\nu\alpha\beta} q^\alpha k^\beta \right) \epsilon_1^{\mu*}(\lambda) \epsilon_2^{\nu*}(\lambda). \quad (\text{A.4})$$

From the decomposition Eq. (A.4) one finds the following relations between the helicity amplitudes and the invariant amplitudes S_1 , S_2 , S_3 :

$$H_0 = -\frac{1}{2\hat{m}_1\hat{m}_2} \left((1 - \hat{m}_1^2 - \hat{m}_2^2) S_1 + \frac{S_2}{2} \lambda(1, \hat{m}_1^2, \hat{m}_2^2) \right), \\ H_\pm = S_1 \pm \frac{S_3}{2} \sqrt{\lambda(1, \hat{m}_1^2, \hat{m}_2^2)}, \quad (\text{A.5})$$

with $\lambda(1, \hat{m}_1^2, \hat{m}_2^2) \equiv (1 - \hat{m}_1^2)^2 - 2\hat{m}_2^2(1 + \hat{m}_1^2) + \hat{m}_2^4$ and $\hat{m}_{1(2)} \equiv m_{1(2)}/m_B$.

Note that the polarized decay amplitudes can be expressed in several different but equivalent bases. For example, the helicity amplitudes can be related to the spin amplitudes in the transversity basis (A_0 , A_\parallel , A_\perp) defined in terms of the linear polarization of the vector mesons via:

$$A_0 = H_0, \quad A_\parallel = \frac{H_+ + H_-}{\sqrt{2}}, \quad A_\perp = \frac{H_+ - H_-}{\sqrt{2}},$$

Table 5 Branching ratio [55], and decay amplitudes for $B_d^0 \rightarrow K^{*0} \rho^0$ [56], $B_d^0 \rightarrow K^{*0} \omega$ [56] and $B_d^0 \rightarrow K^{*0} \phi$, $B_d^0 \rightarrow K^{*0} J/\psi$, $B_d^0 \rightarrow K^{*0} \psi(2S)$ [55].

V	ρ^0	ω	ϕ	J/ψ	$\psi(2S)$
$10^6 \text{BR}(B_d^0 \rightarrow K^{*0} V)$	3.4	2.0	9.8	1330	610
$ h_0^V ^2$	0.70	0.75	0.480	0.570	0.46
$ h_\perp^V ^2$	0.14	0.12	0.24	0.219	0.30
$\arg(h_\parallel^V/h_0^V)$ (rad)	1.17	1.79	2.40	-2.86	-2.8
$\arg(h_\perp^V/h_0^V)$ (rad)	1.17	1.82	2.39	3.01	2.8
$10^4 S_1^V $	1.17	0.81	2.66	33.64	28.86
$10^4 S_2^V $	2.65	1.67	5.20	42.49	52.65
$10^4 S_3^V $	2.31	1.64	5.28	115.28	153.00
$\delta_1^V - \delta_0^V$ (rad)	1.17	1.79	2.40	-2.86	-2.8
$\delta_2^V - \delta_0^V$ (rad)	-2.11	-1.53	-0.84	0.90	1.62
$\delta_3^V - \delta_0^V$ (rad)	1.17	1.82	2.39	3.01	2.8

$A_0, A_\parallel, A_\perp$ are related to S_1, S_2 and S_3 of Eq. (A.1) via

$$A_0 = -\frac{1}{2\hat{m}_1\hat{m}_2} \left((1 - \hat{m}_1^2 - \hat{m}_2^2) S_1 + \frac{S_2}{2} \lambda(1, \hat{m}_1^2, \hat{m}_2^2) \right),$$

$$A_\parallel = \sqrt{2} S_1, \quad A_\perp = \sqrt{\frac{\lambda(1, \hat{m}_1^2, \hat{m}_2^2)}{2}} S_3. \quad (\text{A.6})$$

The amplitude \bar{A}_λ ($\lambda = 0, \parallel, \perp$) are related to the invariant amplitudes of the $\bar{B} \rightarrow \bar{V}_1 \bar{V}_2$ decay by the formulas

$$\bar{A}_0 = -\frac{1}{2\hat{m}_1\hat{m}_2} \left((1 - \hat{m}_1^2 - \hat{m}_2^2) \bar{S}_1 + \frac{\bar{S}_2}{2} \lambda(1, \hat{m}_1^2, \hat{m}_2^2) \right),$$

$$\bar{A}_\parallel = \sqrt{2} \bar{S}_1, \quad \bar{A}_\perp = -\sqrt{\frac{\lambda(1, \hat{m}_1^2, \hat{m}_2^2)}{2}} \bar{S}_3. \quad (\text{A.7})$$

If the $B \rightarrow V_1 V_2$ decay is invariant under CP transformation, then $\bar{A}_0 = A_0$, $\bar{A}_\parallel = A_\parallel$, and $\bar{A}_\perp = -A_\perp$.

The decay width is expressed as follows:

$$\Gamma(B \rightarrow V_1 V_2) = \frac{m_B \sqrt{\lambda(1, \hat{m}_1^2, \hat{m}_2^2)}}{16\pi} \left(\frac{G_F m_B^2}{\sqrt{2}} |V_{CKM}| \right)^2 \times (|A_0|^2 + |A_\parallel|^2 + |A_\perp|^2). \quad (\text{A.8})$$

The matrix element for the $B_d^0 \rightarrow K^{*0} V$ decay, where $V = \rho^0, \omega, \phi, J/\psi(1S), \psi(2S), \dots$ mesons, we can represent as

$$\mathcal{M} = \frac{G_F m_B^3}{\sqrt{2}} |V_{tb}^* V_{ts}| \left(S_1^V g_{\mu\nu} + \frac{S_2^V}{m_B^2} p_\mu p_\nu - i \frac{S_3^V}{m_B^2} \varepsilon_{\mu\nu\alpha\beta} q^\alpha k^\beta \right) \epsilon_1^{\mu*} \epsilon_2^{\nu*}. \quad (\text{A.9})$$

Next, we define the normalized amplitudes:

$$h_\lambda \equiv \frac{A_\lambda}{\sqrt{\sum_{\lambda'} |A_{\lambda'}|^2}},$$

$$\sum_\lambda |h_\lambda|^2 = 1 \quad (\lambda, \lambda' = 0, \parallel, \perp). \quad (\text{A.10})$$

By putting $m_1 = m_V$, $m_2 = m_{K^*}$ and using (A.8), (A.10) we obtain the relation between the amplitudes h_λ and A_λ of the process under study $B_d^0 \rightarrow K^{*0} V$ for any vector meson $V = \rho^0, \omega, \phi, J/\psi(1S), \psi(2S), \dots$:

$$h_\lambda^V = \frac{G_F m_B^2}{4\sqrt{2}} |V_{tb}^* V_{ts}| \sqrt{\frac{m_B \tau_B}{\pi \text{BR}(B_d^0 \rightarrow K^{*0} V)}} \times \lambda^{1/4}(1, \hat{m}_V^2, \hat{m}_{K^*}^2) A_\lambda^V, \quad (\text{A.11})$$

where $\text{BR}(\dots)$ is the branching ratio of $B_d^0 \rightarrow K^{*0} V$ decay and τ_B is the lifetime of a B meson.

Solving Eqs. (A.6) we find the scalars S_1, S_2 and S_3 , and then extend the helicity amplitudes A_λ^V off the mass shell of the meson V , i.e. for $q^2 \neq m_V^2$. We introduce the phases $\delta_\lambda^V \equiv \arg(h_\lambda^V)$, $\delta_i^V \equiv \arg(S_i^V)$, where $i = 1, 2, 3$. Then we have

$$|S_1^V| = \frac{|A_\parallel^V|}{\sqrt{2}}, \quad |S_3^V| = \sqrt{\frac{2}{\lambda(1, \hat{m}_V^2, \hat{m}_{K^*}^2)}} |A_\perp^V|,$$

$$|S_2^V| = \frac{\sqrt{2}}{\lambda(1, \hat{m}_V^2, \hat{m}_{K^*}^2)} \left(8\hat{m}_{K^*}^2 \hat{m}_V^2 |A_0^V|^2 + (1 - \hat{m}_V^2 - \hat{m}_{K^*}^2)^2 |A_\parallel^V|^2 + 4\sqrt{2} \hat{m}_{K^*} \hat{m}_V (1 - \hat{m}_V^2 - \hat{m}_{K^*}^2) \times |A_0^V| |A_\parallel^V| \cos(\delta_\parallel^V - \delta_0^V) \right)^{1/2},$$

$$\sin(\delta_2^V - \delta_0^V) = -\frac{\sqrt{2}}{|S_2^V| \lambda(1, \hat{m}_V^2, \hat{m}_{K^*}^2)} \times (1 - \hat{m}_V^2 - \hat{m}_{K^*}^2) |A_\parallel^V| \sin(\delta_\parallel^V - \delta_0^V),$$

$$\cos(\delta_2^V - \delta_0^V) = -\frac{\sqrt{2}}{|S_2^V| \lambda(1, \hat{m}_V^2, \hat{m}_{K^*}^2)} \times \left((1 - \hat{m}_V^2 - \hat{m}_{K^*}^2) |A_\parallel^V| \cos(\delta_\parallel^V - \delta_0^V) + 2\sqrt{2} \hat{m}_V \hat{m}_{K^*} |A_0^V| \right),$$

$$\delta_1^V \equiv \delta_\parallel^V \pmod{2\pi}, \quad \delta_3^V \equiv \delta_\perp^V \pmod{2\pi}. \quad (\text{A.12})$$

References

1. M. Antonelli *et al.*, Phys. Rep. **494**, 197 (2010)
2. D. Melikhov, N. Nikitin, S. Simula, Phys. Lett. B **442**, 381 (1998)
3. F. Krüger, L.M. Sehgal, N. Sinha, R. Sinha, Phys. Rev. D **61**, 114028 (2000) [Erratum-ibid. D **63**, 019901 (2001)]
4. A. Ali, P. Ball, L.T. Handoko, G. Hiller, Phys. Rev. D **61**, 074024 (2000)
5. C.S. Kim, Y.G. Kim, C.-D. Lu, T. Morozumi, Phys. Rev. D **62**, 034013 (2000)
6. A. Ali, E. Lunghi, C. Greub, G. Hiller, Phys. Rev. D **66**, 034002 (2002)
7. F. Krüger, J. Matias, Phys. Rev. D **71**, 094009 (2005)
8. E. Lunghi, J. Matias, JHEP **0704**, 058 (2007)
9. C. Bobeth, G. Hiller, G. Piranishvili, JHEP **0807**, 106 (2008)
10. C. Bobeth, G. Hiller, D. van Dyk, JHEP **1007**, 098 (2010)
11. C. Bobeth, G. Hiller, D. van Dyk, JHEP **1107**, 067 (2011)
12. U. Egede, T. Hurth, J. Matias, M. Ramon, W. Reece, JHEP **0811**, 032 (2008)
13. W. Altmannshofer, P. Ball, A. Bharucha, A. J. Buras, D. M. Straub, M. Wick, JHEP **0901**, 019 (2009)
14. A. Y. Korchin, V. A. Kovalchuk, Phys. Rev. D **82**, 034013 (2010)
15. U. Egede, T. Hurth, J. Matias, M. Ramon, W. Reece, JHEP **1010**, 056 (2010)
16. E. Lunghi, A. Soni, JHEP **1011**, 121 (2010)
17. A. Bharucha, W. Reece, Eur. Phys. J. C **69**, 623 (2010)
18. A. K. Alok, A. Dighe, D. Ghosh, D. London, J. Matias, M. Nagashima, A. Szynekman, JHEP **1002**, 053 (2010)
19. A. K. Alok, A. Datta, A. Dighe, M. Duraisamy, D. Ghosh, D. London, S. U. Sankar, JHEP **1111**, 121 (2011)
20. A. K. Alok, A. Datta, A. Dighe, M. Duraisamy, D. Ghosh, D. London, JHEP **1111**, 122 (2011)
21. S. Descotes-Genon, D. Ghosh, J. Matias, M. Ramon, JHEP **1106**, 099 (2011)
22. D. Becirevic, E. Schneider, Nucl. Phys. B **854**, 321 (2012)
23. W. Altmannshofer, P. Paradisi, D. M. Straub, arXiv:1111.1257 [hep-ph]
24. A. Y. Korchin, V. A. Kovalchuk, arXiv:1111.4093 [hep-ph]
25. J. Matias, F. Mescia, M. Ramon, J. Virto, arXiv:1202.4266 [hep-ph]
26. D. Das, R. Sinha, arXiv:1202.5105 [hep-ph]
27. D. Das, R. Sinha, arXiv:1205.1438 [hep-ph]
28. M. Beneke, G. Buchalla, M. Neubert, C. T. Sachrajda, Phys. Rev. Lett. **83**, 1914 (1999)
29. M. Beneke, G. Buchalla, M. Neubert, C. T. Sachrajda, Nucl. Phys. B **591**, 313 (2000)
30. M. Beneke, T. Feldmann, D. Seidel, Nucl. Phys. B **612**, 25 (2001)
31. M. Beneke, T. Feldmann, D. Seidel, Eur. Phys. J. C **41**, 173 (2005)
32. B. Grinstein, D. Pirjol, Phys. Rev. D **70**, 114005 (2004)
33. M. Beylich, G. Buchalla, Th. Feldmann, Eur. Phys. J. C **71**, 1635 (2011)
34. A. Khodjamirian, Th. Mannel, A. A. Pivovarov, Y.-M. Wang, JHEP **1009**, 089 (2010)
35. N.G. Deshpande, J. Trampetic, K. Panose, Phys. Rev. D **39**, 1461 (1989)
36. C.S. Lim, T. Morozumi, A.I. Sanda, Phys. Lett. B **218**, 343 (1989)
37. A. Ali, T. Mannel, T. Morozumi, Phys. Lett. B **273**, 505 (1991)
38. Z. Ligeti, M.B. Wise, Phys. Rev. D **53**, 4937 (1996)
39. Z. Ligeti, I.W. Stewart, M.B. Wise, Phys. Lett. B **420**, 359 (1998)
40. F. Krüger, L.M. Sehgal, Phys. Lett. B **380**, 199 (1996)
41. M. Beneke, G. Buchalla, M. Neubert, C.T. Sachrajda, Eur. Phys. J. C **61**, 439 (2009)
42. G. Valencia, Phys. Rev. D **39**, 3339 (1989)
43. I. Dunietz, H. Quinn, A. Snyder, W. Toki, H.J. Lipkin, Phys. Rev. D **43**, 2193 (1991)
44. A. S. Dighe, I. Dunietz, H. J. Lipkin, J. L. Rosner, Phys. Lett. B **369**, 144 (1996)
45. B. Aubert *et al.* (BABAR Collaboration), Phys. Rev. Lett. **98**, 051801 (2007)
46. B. Aubert *et al.* (BABAR Collaboration), Phys. Rev. D **78**, 092008 (2008)
47. P. Ball, R. Zwicky, Phys. Rev. D **71**, 014029 (2005)
48. N. Cabibbo, Phys. Rev. Lett. **10**, 531 (1963).
49. M. Kobayashi, T. Maskawa, Prog. Theor. Phys. **49**, 652 (1973)
50. R.P. Feynman, *Photon-hadron interactions*, (W.A. Benjamin, Inc. Reading, Massachusetts, 1972)
51. F. Klingl, N. Kaiser, W. Weise, Z. Phys. A **356**, 193 (1996)
52. H.B. O'Connell, B.C. Pearce, A.W. Thomas, A.G. Williams, Prog. Nucl. Part. Phys. **39**, 201 (1997)
53. G. Ecker, J. Gasser, A. Pich, E. de Rafael, Nucl. Phys. B **321**, 311 (1989)

54. S. Eidelman, S. Ivashyn, A. Korchin, G. Pancheri, O. Shekhovtsova, *Eur. Phys. J. C* **69**, 103 (2010)
55. K. Nakamura *et al.* (Particle Data Group), *J. Phys. G* **37**, 075021 (2010)
56. C.H. Chen, arXiv:hep-ph/0601019
57. J. T. Wei *et al.* (BELLE Collaboration), *Phys. Rev. Lett.* **103**, 171801 (2009)
58. T. Aaltonen *et al.* (CDF Collaboration), *Phys. Rev. Lett.* **107**, 201802 (2011)
59. T. Aaltonen *et al.* (CDF Collaboration), arXiv:1108.0695 [hep-ex]
60. R. Aaij, *et al.* (LHCb Collaboration), arXiv:1112.3515 [hep-ex]
61. G. Buchalla, G. Isidori, S.-J. Rey, *Nucl. Phys. B* **511**, 594 (1998)
62. T. Hurth, M. Nakao, *Ann. Rev. Nucl. Part. Sci.* **60**, 645 (2010)
63. B. Aubert *et al.* (BABAR Collaboration), *Phys. Rev. Lett.* **93**, 081802 (2004)
64. M. Iwasaki *et al.* (BELLE Collaboration), *Phys. Rev. D* **72**, 092005 (2005)